Surface Science 124 (1983) 461–488
North-Holland Publishing Company

THEORY OF CHARGE TRANSFER FOR DESORPTION OF IONS FROM SURFACES

B.J. GARRISON *, A.C. DIEBOLD ** and J.-H. LIN

Department of Chemistry, The Pennsylvania State University, University Park, Pennsylvania 16802, USA

and

Z. SROUBEK

Institute of Radio Engineering and Electronics, Czechoslovak Academy of Sciences, Prague 8, Lumumbova 1, Czechoslovakia

Received 21 September 1982

A microscopic model is presented to describe the probability of charge transfer for the desorption of ions from surfaces. The model explicitly incorporates the electronic structure of the system by including orbitals for each atom that interact via a time dependent hopping integral. This prescription also takes into account the motion of the nuclei which may occur in conjunction with energetic ion bombardment. As a consequence, the model is three-dimensional in nature and incorporates the electronic structure of the system at the time of desorption of the atom. The initial motions studied are ones where the adsorbate atom desorbs perpendicularly to the surface with a given velocity, v. For this motion and velocities less than $\sim 10^6$ cm/s we find that the ionization probability R^+ is proportional to v^n with n between 2 and 4. For higher velocities R^+ can depend more exponentially on $(-\text{const.}/v)$. The effect of the various parameters in the model including the atomic orbital energies, the coupling strength and effective range, and the assumed motion of the desorbing atom are examined in detail. The relevance of this model to a fundamental understanding of SIMS experiments is also stressed.

1. Introduction

The desorption of energetic particles from solids has attracted considerable interest as a means of determining the original atomic composition and geometry of the surface. For example, ion bombardment techniques such as secondary ion mass spectrometry (SIMS) can detect 0.01 of a monolayer of atomic species on the surface [1]. SIMS, fast atom bombardment mass spec-

* Alfred P. Sloan Research Fellow.
** Present address: Allied Corporation, Morristown, New Jersey, USA.

0039-6028/83/0000-0000/$03.00

trometry (FABMS) and ^{252}Cf plasma desorption mass spectrometry (^{252}Cf PDMS) have been quite successful in desorbing high mass (1000–20,000 amu) molecules from a surface thus allowing their mass spectra to be obtained [2]. The highly anisotropic angular distributions of particles desorbed during SIMS [3] or electron or photon stimulated desorption (ESD or PSD) [4] experiments have been interpreted as being directly related to the bonding geometry of atoms on a surface. Techniques such as MeV Rutherford backscattering [5] or ion scattering spectrometry (ISS) [6] also make use of angular distributions of reflected ions to determine surface structures.

To make precise determinations, either of the quantitative composition of elements on the surface or of exact bonding geometries, the mechanism of desorption, both for the nuclear and electronic motion, needs to be understood in detail. Although considerable effort has been expended in trying to understand the nuclear motion of the desorbing particles [2,7], relatively little is understood about the basic processes involved in the ionization (neutralization), particularly at the microscopic level. Besides a need to grasp a fundamental understanding of the process, a prescription for interpretation of the experimental data is also necessary. In the ion bombardment experiments the ion yields are extremely sensitive to the original matrix. In general, electron withdrawing species like oxygen tend to enhance by orders of magnitude positive ion yields and suppress negative ion yields, while electron donating elements such as cesium have the reverse effect. However, to complicate the interpretation, addition of oxygen to a silicon solid has been found to enhance both the Si^- and Si^+ intensities by 1–2 orders of magnitude [8]. Obviously the electronic structure as described by the macroscopic quantities of work function, ionization potential and electron affinity has a strong effect on the charge state and intensity of the ejected species. When examining angular distributions then of desorbed ions in SIMS or ESD it is not clear whether the ionization and/or neutralization process is independent of angle of ejection.

Much of the problem in being able to analyze theories of ionization and/or neutralization processes stems from the shortage of detailed experimental data. Lundquist has measured the energy distributions of Cu^0 and Cu^+ particles ejected from clean copper due to ion bombardment [9]. Unfortunately he was only able to measure relative intensities averaged over all angles of ejection. He did find, however, that the ionization probability depended approximately linearly on velocity.

Recently angle resolved SIMS measurements by Gibbs et al. have been made for Ni^+ ions observed to eject from a CO covered Ni(001) surfaces [3]. The data were obtained at a variety of ejection angles and energies. Quantitative comparisons of the angular distributions of the ejected particles between these data and a classical dynamics model which predicts the yield of ejected neutral atoms could be obtained if the ionization process is assumed to be independent of angle and energy of the ejected nickel atom and if the

trajectory of the ion compared to the neutral is influenced only by an image force set up in the solid. Again these data imply that the ionization probability is only weakly dependent on energy.

Yu has recently measured the velocity dependence of O^- ions ejected from vanadium and niobium surfaces as a function of work function and ejection velocity and angle [10]. For perpendicular velocities $v_\perp$ of ejection between 1×10^6 and 3×10^6 cm/s he finds that the ion yield is proportional to $\exp(-\text{const.}/v_\perp)$. For lower velocities the ion yield does not depend as strongly on $v_\perp$. In these experiments the ionization probability is more strongly dependent on velocity than in either of the previous two studies.

Recent experiments by Winograd, Baxter and Kimock in which the ejected neutral atoms are ionized by multiphoton resonance ionization seem very promising for obtaining the experimental data necessary for making detailed comparisons of ion and neutral yields [11]. This technique should ultimately be able to provide energy and angular distributions of both the ejected neutrals and ions. The data at this stage are preliminary, however, and are not sufficiently detailed for comparisons with microscopic theories.

The current theories for the ionization process are reviewed in recent articles by Williams [8] and Tolk and Tully [12]. The majority of these theories and models are analytic and as a consequence are one-dimensional in form. The precise dynamics of the nuclei giving rise to the ejection of the atom is generally not taken into account. Particularly in the bombardment experiments, the electronic structure at the time of ejection is surely different from that of the original quiescent surface. In addition there will be several types of collision sequences that give rise to an ion ejected at a specific angle and velocity [13]. Thus, a three-dimensional model that takes into account the nuclear dynamics as well as the local electron environment seems most appropriate.

In this study a model is presented that incorporates the electronic motion into a well developed scheme of following the nuclear motion of the atoms. In this precription the electronic levels of the systems are described explicitly. The wavefunctions in the solid are expressed as a linear combination of atomic orbitals. First order differential equations can be derived for the time dependent expansion coefficients. These equations are then numerically integrated along with Hamilton's equations for the nuclear motion to determine the final ionization probability. This model has been used in various forms by other groups to describe ion and neutral scattering from solids [14–17] and the ejection of ions from solids due to ion bombardment [18,19]. Sroubek has analytically solved the coupled equations for the special case of only two electronic levels [20]. Other workers have approximated the solution for an infinite set of substrate levels assuming the substrate remains static [15,21]. Finally, Sroubek, Zdansky and Zavadil have numerically solved the coupled equations for a solid of six atoms [22]. The previous solutions offer limiting

cases with which the results of this study can be compared. The results of the various analytic solutions are briefly described below.

In the limit of two levels, one level for the substrate and one for the atom or adatom which desorbs, the ionization probability R^+ for the ejected atom can be determined analytically. Here the adatom has a single time independent level ϕ_a of energy ϵ_a that interacts with the single time independent metal substrate level ϕ_i of energy ϵ_i. The energy ϵ_a is assumed to be less than ϵ_i. The electron, then, initially resides in ϕ_a on the adatom with the level ϕ_i unoccupied. If the time dependent coupling (hopping integral) $V(t)$ between the levels is slowly turned on, then the ionization probability R^+ can be calculated from perturbation theory [20,23]. The slow turn on of the coupling is equivalent to bringing the adatom up to the substrate with an infinitely slow velocity. Sroubek [20] determined for

$$V(t) = V_0 \, e^{-\lambda v t}, \quad t \geq 0, \tag{1}$$

that

$$R^+ = \hbar^2 v^2 \lambda^2 V_0^2 / \left\{ (\epsilon_i - \epsilon_a)^2 \left[\hbar^2 v^2 \lambda^2 + (\epsilon_i - \epsilon_a)^2 \right] \right\}, \tag{2a}$$

where V_0 is the strength of the interaction at $t = 0$, λ is the effective range of the interaction, v is the relative velocity of the two atoms and $\hbar$ is Planck's constant devided by 2π. In the low velocity limit R^+ is proportional to v^2 and at high velocities

$$\lim_{v \to \infty} R^+ \sim V_0^2 / (\epsilon_i - \epsilon_a)^2. \tag{2b}$$

For $V_0 \ll (\epsilon_i - \epsilon_a)$, eq. (2b) yields the partial charge on the adatom at $t = 0$. Diestler [24] has recently obtained an identical expression for R^+ as given in eq. (2) by using a molecular orbital rather than atomic orbital basis. With his formalism it is not necessary to slowly turn on the coupling. His model seems physically more appropriate for the desorption process because undoubtedly the initial electronic configuration more closely resembles molecular orbitals rather than atomic orbitals. He also assumed, however, that the initial charge on the adatom was small ($V_0 \ll (\epsilon_i - \epsilon_a)$). The results presented here show that the approximation that the electron is initially on the adatom is the most stringent. In a practical sense, $R^+(t = 0) \lesssim 0.1$ must be achieved before the analytic expression of eq. (2) is valid. This seems too severe for real systems. For the covalent molecule HCl, the initial charge separation is $\sim 0.1 \rightarrow 0.2$ of an electron. One would expect this range of partial charges to be most reasonable for chemisorbed atoms or molecules on surfaces.

Several workers have applied the same basic formalism to the scattering of ions from surfaces in order to predict the neutralization probability [15,21]. For an infinite set of levels in the solid and the functional form of $V(t)$ in eq. (1) the problem can be solved analytically. Assuming a static solid they obtain

$$R^+ = (2/\pi) \exp\left[-\pi (\mathrm{IP} - \phi) / \hbar \lambda v \right], \tag{3}$$

where $IP \simeq -\epsilon_a$ is the ionization potential of the adatom and ϕ is the work function of the substrate [25]. Note that eq. (3) has a very different velocity, λ, and $(IP - \phi)$ dependence than eq. (2) and exhibits no V_0 dependence.

Nørskov and Lundqvist [21] as well as Sroubek [20] have pointed out that eq. (3) predicts too strong a velocity dependence of R^+ for the ejection process. For reasonable values of the parameters in eq. (3) the ionization probability of sodium atoms varies by 20 orders of magnitude as the energy increases from 1 to 100 eV. Eq. (3) however has certain appeal because it can be related to the Local Thermal Equilibrium (LTE) [26] expression of ionization where

$$R^+ \propto \exp\left[-(IP - \phi)/kT_{eff}\right], \tag{4}$$

by

$$kT_{eff} = \hbar\lambda v/\pi. \tag{5}$$

The LTE expression has been used to fit experimental data quite successfully although the interpretation of the physical meaning of T_{eff} is open to discussion [8,12]. Nørskov and Lundqvist adjust eq. (3) on the basis that the adsorbate level ϵ_a will vary as the adatom departs from the surface. However, they keep the basic functional form of eq. (3). They obtain

$$R^+ = (2/\pi)\exp\left[-C_1\pi(IP - \phi)/\hbar\lambda v\right] \tag{6}$$

where C_1 is a fitting parameter [21].

Finally, Sroubek, Zdansky and Zavadil have numerically solved the Schrödinger equation and the atomic equations of motion for a solid of six atoms with a total of eleven electronic levels and found that R^+ was virtually independent of velocity [20,22]. Here the atoms in the solid were allowed to move as the adatom desorbed from the surface. Only one collision sequence for each velocity of the ejected atom, however, was examined.

Our goal then is to incorporate the microscopic model for the ionization process into our well developed classical dynamics procedure for following the nuclear motion [7]. Ultimately it is desirable to predict the ionization probability of an atom desorbing from the surface with a specific velocity and at a given angle. In general, however, several collision sequences in the solid will give rise to the desorption of an atom with the desired properties. Preliminary calculations where motion in the solid has been included yielded results that were difficult to interpret since variations in the velocity of the ejected adatom were also associated with the variations in the angle of ejection and with the motion of atoms in the solid [7]. Thus two simpler systems were chosen to examine initially. The first system is the two-level model. Here the results can be compared to the analytic results of eq. (2) and used to determine the validity of the approximations assumed in the derivation of eq. (2). The second system is one where many electronic levels are included but the nuclear motion of atoms is restricted. The initial nuclear motions that are examined are ones

where the adatom is given an arbitrary velocity perpendicular to the surface. Although in principle the remainder of the atoms in the solid can move, they remain stationary due to the initial conditions. This scheme is most closely comparable to ESD or PSD experiments, rather than to ion bombardment experiments. The conditions of the calculation, however, are similar to all other analytic theories for charge exchange since they assume a static solid and a perpendicular component of velocity in the expression of R^+. This desorption calculation also allows one to examine the effect of the various assumed parameters in the model on the predicted values of R^+.

One of the primary concerns in using this model is whether it will be computationally feasible to include as many atoms and/or levels in the solid so that an experimental system is realistically reproduced. For this specific set of desorption adatom motions, convergence can be obtained with respect to the number of atoms in the solid in the values of R^+ with 9 atoms, each with two electronic levels. The convergence with respect to the number of levels per atom is not as good as for the previous case although the overall dependence of R^+ on velocity does not change dramatically. Surprisingly, however, the results from the calculations are qualitatively very similar to those obtained by using only two levels.

In sections 2 and 3 the model and description of the calculation are presented. The results of the two-level and multilevel calculations for the desorption process are described in section 4. For both systems the parameters v, V_0, λ, and ϵ_a are systematically varied to determine their influence on R^+. In addition, a different functional form of $V(t)$ is examined in order to determine the sensitivity of the results to the assumed electronic interaction. Initial results are also presented where the adatom is desorbed due to a collision with a substrate atom.

2. Model

The ionization process for ejected adatoms is modeled using a classical path method. The Hamiltonian is separated into a part for the motion of the atomic nuclei in the system (adatom, metal substrate atoms), and a part for the electronic motion. The nuclear motion is presumed to be correctly described by classical mechanics, thus a molecular dynamics simulation is used to obtain the time dependent atomic positions required for the solution of the electronic Hamiltonian. This means that the nuclear motions are unaffected by the electronic transitions that occur during the trajectory. For a further discussion of the assumptions made by the classical path method, the reader is referred to the recent review by Tully [27].

One determines the ionization probability of the adatom by solving the time dependent electronic Hamiltonian. We choose to describe the system by the

one-electron tight binding approximation. This electronic Hamiltonian has been formulated in a metal "band", adsorbate orbital and in an atomic site representation. The atomic site representation is a more useful representation for classical path simulations because the atoms often move from their original ordered positions. Metal–metal electronic excitations can be included in a more transparent fashion since we need not follow the excitation of metal bands during a process that destroys lattice periodicity. The Hamiltonian is considered to be

$$H = H_{\mathrm{at}} + U(\boldsymbol{r}(t)), \tag{7}$$

where H_{at} is an atomic Hamiltonian, U is a time or position dependent interatomic electronic interaction and $\boldsymbol{r}$ is a vector of the positions between the nuclei. The coupling U neglects electron–electron interactions, thus no two-electron or Auger-type processes are considered.

The solutions to the atomic Hamiltonian H_{at} are given by time independent, orthonormal, atomic wavefunctions ϕ_k, of energy ϵ_k where

$$H_{\mathrm{at}}\phi_k = \epsilon_k \phi_k. \tag{8}$$

For the studies presented here the adatom is assumed to have one level ϕ_a of energy ϵ_a, thus electronic excitations within the adatom are neglected.

We now seek time dependent molecular wavefunctions ψ_i where

$$H\psi_i = \mathrm{i}\hbar\,\partial\psi_i/\partial t. \tag{9}$$

The wavefunction ψ_i is expanded in a linear combination of atomic basis functions with eigenvalues E_i as

$$\psi_i = \sum_j \phi_j c_{ji}(t)\exp(-\mathrm{i}E_i t/\hbar), \tag{10}$$

where an arbitrary phase factor has been included. Substituting ψ_i from eq. (10) into eq. (9), multiplying on the left by ϕ_k^* and integrating over the electronic coordinates yields the following coupled equations,

$$\mathrm{i}\hbar\,\mathrm{d}c_{ki}(t)/\mathrm{d}t = \sum_j \langle\phi_k|U|\phi_j\rangle\, c_{ji}(t) - E_i\, c_{ki}(t). \tag{11}$$

These equations of motion for the expansion coefficients $c_{ki}(t)$ can be integrated simultaneously with Hamilton's equations for the nuclear motion. The initial conditions for $c_{ki}(t=0)$ are found by setting eq. (11) equal to zero. This results in the stationary state eigenvalue–eigenvector equation.

In this work the following form of the coupling matrix element or hopping integral is used and given by

$$\begin{aligned}\langle\phi_k|U|\phi_j\rangle &= V(r(t)) \\ &= V_0^{kj}\exp\left[-\lambda_{kj}\left(r_{kj}(t) - r_{kj}^{\mathrm{e}}\right)\right],\end{aligned} \tag{12}$$

where k and j are associated with different atoms

$$= \begin{cases} \epsilon_k, & k = j, \\ 0, & k \neq j, \end{cases}$$

where k and j are associated with the same atom.

The exponential form for V has been used extensively in both analytic theories of ionization by sputtering and desorption and in previous classical path calculations [14–22]. This equation is identical to eq. (1) if the atoms move apart with a constant velocity v from an initial separation r^e. This exponential form can be related to the overlap of two atomic wavefunctions.

The ionization probability is calculated from the coupling coefficients in the following manner: (1) Choose some atomic energies ϵ_k and parameters for the coupling element $V(r)$. (2) Obtain, by solving eq. (11) set equal to zero, the molecular energies E_i and the initial values of the expansion coefficients $c_{ki}(t=0)$. (3) Determine the nuclear motion of the total system by the molecular dynamics method described below. At each timestep in the molecular dynamics, the new nuclear positions serve as input to the coupling matrix element, eq. (12). The coupled equations of motion for the $c_{ki}(t)$ are simultaneously integrated with the nuclear positions and momenta. (4) Evaluate the ionization probability R^+ of the adatom at the end of the desorption process by

$$R^+ = \sum_i^{\text{unocc}} |c_{ai}(t=\infty)|^2, \tag{13}$$

where c_{ai} is coefficient of adatom in the ith molecular orbital and the sum is only over those molecular states that were originally unoccupied. Bu unitarity R^+ can also be defined as

$$R^+ = 1 - \sum_i^{\text{occ}} |c_{ai}(t=\infty)|^2, \tag{14}$$

where now the sum is over the occupied molecular states.

3. Description of the model systems

In this paper we investigate an ensemble of atoms consisting of a single adatom adsorbed on a collection of substrate atoms. The adatom is given an arbitrary velocity perpendicular to the surface causing it to desorb. Both the adatom and substrate atoms have atomic orbitals that electronically interact. The first calculations employ one substrate atom and one adatom placed initially at their equilibrium distance and then moved apart with a constant velocity. This situation assumes that only one electronic level from each the

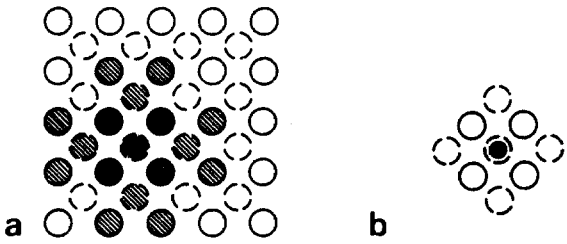

Fig. 1. Cu(001): (a) The 25 solid line circles represent top layer atoms and the 16 dashed line circles represent second layer atoms. The one solid disk near the center is the adatom. The five circles hatched in both directions are the atoms designated zone E in the text. Zone G has 17 metal atoms which include zone E plus the remainder of the hatched atoms. (b) Zone F.

adsorbate and substrate are involved in the electron transfer. This system is then extended to include many interacting levels. Finally, for one of the multilevel systems, the motion of the adatom is initiated by a collision from within the substrate. This motion is started by striking the bottom of the crystal with a particle several layers beneath the adatom. By this procedure the direction of ejection of the adatom can be fixed normal to the surface yet at the same time the adatom's motion is initiated smoothly in a manner more analogous to desorption due to ion bombardment.

For the present study, copper is chosen for the substrate since (i) we have had previous experience with the dynamics on this system [7], and (ii) it is monovalent with the configuration $3d^{10}4s^1$ and is amenable to treatment as a one-electron atom. The adatom is assumed to have the interaction potentials and mass appropriate for oxygen. The range of adsorbate energies ϵ_a used, however, is more indicative of the ionization potentials of the alkali metals.

The nuclear motion of the adatom and metal atoms is determined by the molecular dynamics procedure described previously [7]. The metal is modeled by a 2 atomic layer microcrystallite that is representative of the Cu(001) surface. The surface size of the crystallite is shown in fig. 1a. This crystal size is larger than actually needed for the desorption dynamics because the metal atoms hardly move from their initial positions. We used this size because of

Table 1
Parameters for the interaction potentials [a]

	A (keV)	B ($Å^{-1}$)	D_e (eV)	β ($Å^{-1}$)	R_e (Å)	R_a (Å)	R_b (Å)	R_c (Å)
Cu–Cu	22.564	5.088	0.48	1.405	2.628	1.500	1.988	4.338
Cu–adsorbate			0.18	2.45	2.06	–	–	4.338

[a] See eqs. (1)–(6) of ref. [13] for the functional forms of the interaction potentials.

concurrent studies underway in which a larger crystal is required. The potential energy among the atoms is assumed to be a sum of pair potentials. The form and description of the potentials can be found in ref. [13] and in table 1 we list the potential parameters used in this study. The adatom is situated in a fourfold bridge site 1 Å above the surface plane.

The first step in determining the ionization probability R^+ is to choose atomic energies for the metal atoms and the adatom, as well as to select parameters for the coupling matrix elements. Since we are supposing a one-electron metal, two electronic levels with energies ϵ_1 and ϵ_2 are assigned to each metal atom. The adatom has one level of energy ϵ_a. Initially attempts were made to choose ϵ_1 and ϵ_2 so that the band width and work function of copper are reasonably well described. The effect of this choice of parameters is that $R^+(t=0)$ varies considerably with the number of electronically interacting levels. As discussed below the value of the initial charge on the adatom influences the predicted values of R^+. Thus with parameters chosen to model the band structure of copper, it is difficult to determine the convergence properties of R^+ as the number of levels increases. Finally we chose parameters so that R^+ $(t=0)$ is reasonably constant with increasing numbers of atoms that interact electronically. The base values of the atomic energies are $\epsilon_1 = -5.5$ eV, $\epsilon_2 = -5.0$ eV and $\epsilon_a = -6.0$ eV. However, only the relative energies are important.

Since we are examining a model system the values for the coupling parameters are arbitrarily selected. The coupling strength V_0 is set equal to 0.20 eV for both the copper–copper and copper–adsorbate interactions. The coupling range, λ, is set equal to 2.3 $Å^{-1}$. Both V_0 and λ, however, are varied in the calculations to test their influence on R^+. The values of r^e are held fixed at 2.56 Å for Cu–Cu interactions and 2.06 Å for the Cu–adsorbate interactions.

In previous calculations of the nuclear motion alone, a low order predictor–corrector integrator is used [28,29]. The ejection process is complete in $\sim 10^{-13}$ s and takes typically 100–200 integration steps. The ionization coefficients $c_{ki}(t)$ vary much more rapidly in time than the nuclear coordinates. Thus, for the ionization process 2000–20,000 integration steps are necessary. We find that by switching to a fifth order predictor–corrector integrator [30], better numerical stability is obtained in the integration procedure. We test for proper integration by comparing the value of R^+ as calculated by eq. (13) to that from eq. (14). The integration is terminated when the value of R^+ no longer changes with time. For the range of parameters that have been examined stabilization typically occurs when the adsorbate is ~ 6 Å above the surface.

If this model is to be eventually employed to realistically examine ionization probabilities for the ion bombardment process, we must carefully assess whether sufficient atoms and levels can be included numerically such that the electronic Hamiltonian of the infinite solid is accurately described. To de-

Table 2
Description of the various electronic zones

Zone	Number of metal atoms	Number of orbitals per metal atom	Orbital energies of each metal atom (eV)	Total number of levels [a]	Total number of electrons
A, B, C [b]	1	1	−5.3	2	1
D	4	1	−5.1	5	1
E	5	2	−5.0, −5.5	11	6
F	9	2	−5.0, −5.5	19	10
G	17	2	−5.0, −5.5	35	18
H	5	3	−4.95, −5.0, −5.5	16	6
I	5	4	−4.95, −5.0, −5.05, −5.5	21	6
J	5	3	−5.0, −5.45, −5.50	16	11
K	5	4	−4.95, −5.0, −5.45, −5.5	21	11

[a] In all cases the adatom has one level of energy $\epsilon_a = -6.0$ eV.
[b] See text for the detailed differences.

termine the convergence of the predicted values of R^+ in the desorption process, various electronic models have been examined. Each model is described by the atoms which have atomic orbitals and electronically interact. Each set of interacting atoms and their levels is referred to as an electronic zone. In all cases the size of the electronic zone is considerably smaller than the total number of atoms included for the nuclear motion. The zones are divided into three basic groups. The zones in the first group, I, are simple extensions of the two-level model. The zones in group II have two orbitals on each metal atom. The various zones have different numbers of metal atoms included. The zones in group III contain five metal atoms each but vary in the number of atomic orbitals per atom. In all cases the adsorbate atom has one level. The characteristics of each zone are summarized in table 2.

The zones in group I are described below.

(A) *Two-level model with no surface binding energy.* In this model the adatom is initially directly above the metal atom with which it interacts. There is no binding energy between the atoms (i.e., the parameter D_e of table 1 is equal to zero), thus the desorption velocity of the adatoms is constant. The energy difference between the levels, 0.7 eV, is chosen such that $R^+(t=0)$ is approximately the same as for the remainder of the zones.

(B) *Two-level model with a surface binding energy.* This model is identical to that described in (A) above except that an attractive interaction of 0.8 eV is

included, thus the desorption velocity of the adatom is not constant, For an atom of mass 16 amu, 0.8 eV corresponds to a velocity of $10^{5.5}$ cm/s.

(C) *Two-level model with a non-zero impact parameter.* This model is similar to that described in (B) except the atoms have a non-zero impact parameter. The adsorbate is initially in the fourfold bridge site, 1.0 Å above the surface (fig. 1). The metal atom with which it interacts is one of the nearest neighbors in the first layer.

(D) *Expanded two-level model.* This model represents a transition between groups I and II. Here the four metal atoms in the first layer neighboring the adatom each have one level of energy −5.1 eV. The adatom has one level of energy −6.0 eV. There is one electron in the entire system. Thus the one unoccupied level in the two-level model has been replaced by four.

There are three models in group II. Each metal atom has two atomic levels of energies −5.0 and −5.5 eV and the absorbate atom has one level of energy −6.0 eV.

(E) *Six-atom model.* Here there are five metal atoms, four in the first layer surrounding the adatom and one in the second layer directly below the adatom. The adatoms are hatched in both directions in fig. 1a. There are 11 electronic levels with 6 electrons.

(F) *Ten-atom model.* Four second layer atoms (fig. 1b) have been added to the model described in (E).

(G) *Eighteen-atom model.* Eight additional first layer atoms have been added to zone F (fig. 1a). A total of 17 metal atoms are included. This results in 35 electronic levels with 18 electrons.

As discussed below, zone F appears to be a reasonable size and is used for most of the calculations. Zone E, although not quantitatively as good, does predict the same characteristics of the dependence of R^+ on velocity. Thus for the zones in group III we have used the same 5 metal atoms as in zone E. Additional atomic levels are included to increase the *density* of molecular levels without adding new levels at significantly different energies. Changing the energy spectrum does alter the predicted ionization probability. In all cases the adatom has one atomic level of energy −6.0 eV.

(H) *Six-atom model with additional unoccupied levels.* An additional unoccupied level of energy −4.95 eV is added to each metal atom of zone E. There is a total of 16 levels and 6 electrons.

(I) *Six-atom model with two sets of additional unoccupied levels.* Two additional unoccupied levels of energies −5.05 and −4.95 eV are added to each metal atom of zone E. This brings the totals to 21 levels and 6 electrons.

(J) *Six-atom model with additional occupied levels.* An occupied level of energy −5.45 eV is included for each metal atom of zone E. There are 16 levels and 11 electrons.

(K) *Six-atom model with additional occupied and unoccupied levels.* Finally, an additional occupied and unoccupied level of energies −5.45 and −4.95 eV are

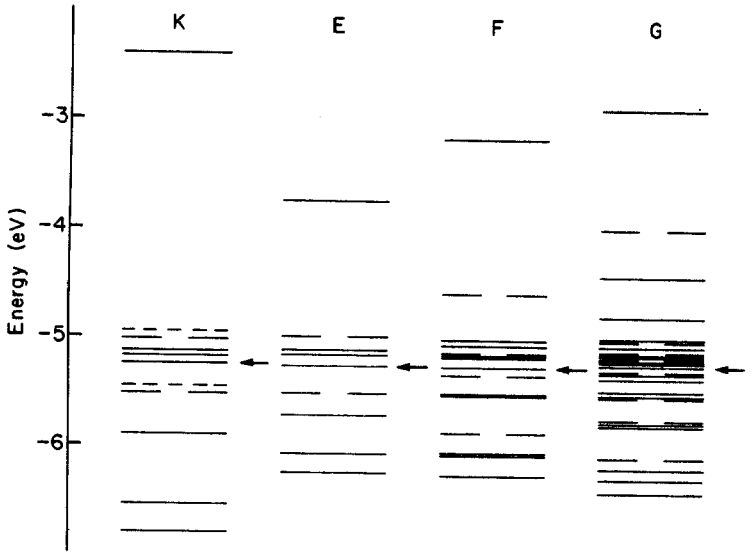

Fig. 2. The energy level diagram for electronic zones E, F, G, and K. The arrow designates the highest occupied level.

added to each metal atom of zone E. This results in 21 levels and 11 electrons.

The molecular energy level diagram is shown in fig. 2 for the electronic zones, E, F, G and K. In each case the arrow denotes the highest occupied level.

4. Results and discussion

The values of the ionization probability R^+ have been examined for velocities of the desorbing adatom between $10^{5.5}$ and 10^8 cm/s. For the exponential coupling integral of eq. (12), the number of levels in the electronic zone, the coupling strength V_0, the coupling range λ and the adatom energy ϵ_a have been varied. The results of these calculations are discussed in subsections 4.1–4.4. The effect of using an alternate coupling integral on the predicted dependence of R^+ on velocity as well as the results from the simulated bombardment motion are examined in subsection 4.5.

4.1. R^+ versus velocity

One of the most critical parameters for interpreting experimental data is the dependence of the ionization probability R^+ on the velocity of the desorbing particle. As discussed in the introduction the various analytic models predict

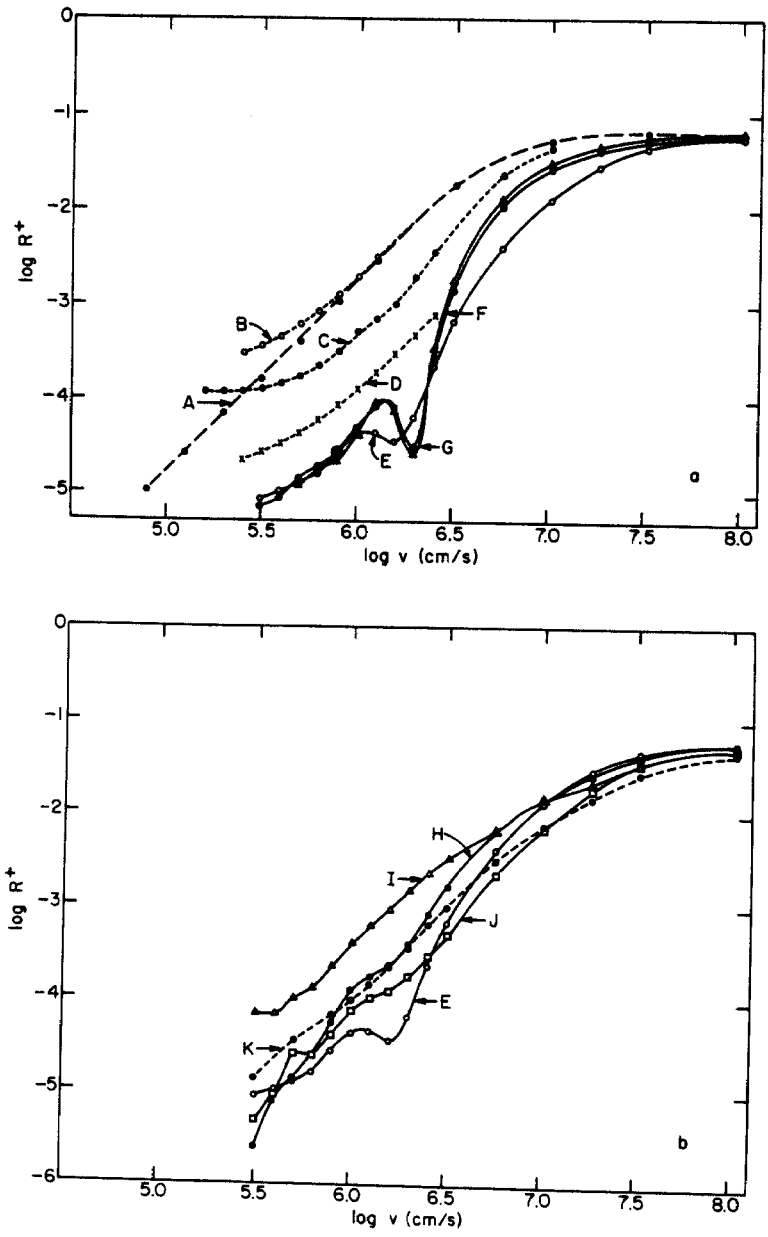

Fig. 3. (a) Log R^+ versus log v for various group I and II electronic zones. The letters designate which zone has been used and are defined in the text. (b) Log R^+ versus log v for various group III electronic zones. The letters designate which zone has been used and are defined in the text.

very different velocity dependences of R^+. Obviously the assumed dependence of R^+ on v will significantly affect the interpretation of experimental data. The calculated values of log R^+ are plotted versus log v in fig. 3a for the various electronic zones in groups I and II described above. For the two-level model (curve A) R^+ is proportional to v^2 for velocities less than $10^{6.5}$ cm/s. Inclusion of attractive forces, both for zero impact (curve B) and non-zero impact (curve C) parameters tends to make R^+ less dependent on the velocity in the low velocity regime. This effect is in qualitative agreement with recent experiments by Yu [10]. As the size of the electronic zone increases (curves D–G) the ionization probability shifts although R^+ is still approximately proportional to v^n with n between 2 and 4 and for velocities $\leqslant 10^{6.5}$ cm/s even with 35 electronic levels (zone G). As the number of levels is increased, however, the dependence of R^+ on $-1/v$ does become more exponential in form for $v \geqslant 10^{6.5}$ cm/s. At large velocities the ionization probability is simply equal to the initial charge on the adatom (sudden limit).

Zones F and G predict almost identical ionization probabilities with zone E yielding the same qualitative features. This is somewhat surprising since the density of the lowest unoccupied levels changes (fig. 2) as the number of atoms is increased. As a reasonable compromise between computer time and accuracy we have chosen zone F as the one to use in the remainder of the calculations. It is somewhat discouraging that 9 metal atoms are needed to describe the desorption of an adatom in the direction normal to the surface. As the angles of ejection become off normal and motion in the solid increases, the number of levels needed will undoubtedly increase [31].

Although the convergence of R^+ with respect to number of metal atoms, each with two levels, is quite good, such convergence with the number of levels per atom could not be obtained. The effect of adding more levels per atom (group III zones) on the log R^+ versus log v curves is shown in fig. 3b. Even though same numerical values of R^+ are not obtained at each velocity the shapes of the curves are not significantly altered. An exponential dependence of R^+ on $-1/v$ is not approached as the number of levels per atom increases. Also note that the minimum in curve E at $\sim 10^{6.2}$ cm/s disappears as the density of levels is altered. As will be discussed later, this is a resonance type effect where the energy difference between two levels approximately equals $\hbar\lambda v$. This structure in the log R^+ versus log v curves then is a consequence of discrete energy levels and would probably not be observed experimentally for a dense spectrum of metal levels. For interactions with discrete levels this type of resonance can be observed [32].

4.2. R^+ versus V_0

Most analytic expressions for the ionization probability are derived using the assumption that initially the electron is primarily on the adatom, thus

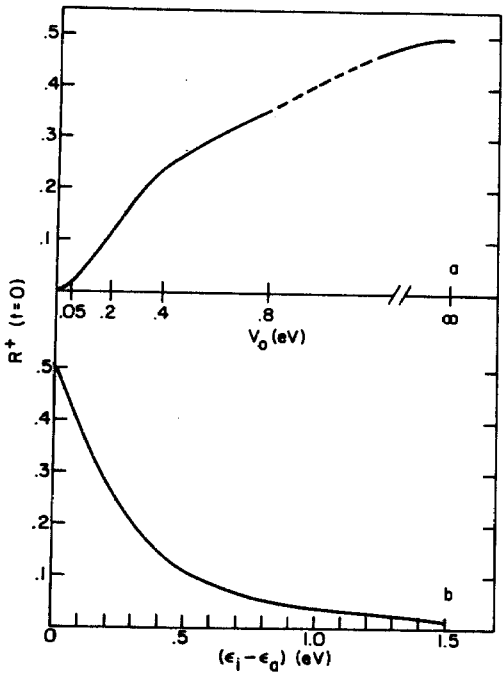

Fig. 4. $R^+(t=0)$ of two-level model versus V_0 for $(\epsilon_i - \epsilon_a) = 0.50$ eV and $\lambda = 2.3$ Å^{-1} (a), and versus $(\epsilon_i - \epsilon_a)$ for $V_0 = 0.20$ eV and $\lambda = 2.3$ Å^{-1} (b).

$R^+(t=0)$ is small. For most covalent molecules and for solids, this assumption is generally not valid. For example, in HCl, a covalent molecule, the charge separation is between 0.1 and 0.2 electron. These values should also be appropriate for chemisorbed species on surfaces. In the two-level numerical model, the initial charge is influenced by two parameters, V_0 and $(\epsilon_i - \epsilon_a)$. The coupling strength V_0 measures how effectively the two levels communicate with each other. With $\epsilon_a < \epsilon_i$ and V_0 small, the electron initially resides in ϕ_a and $R^+(t=0) \simeq [V_0/(\epsilon_i - \epsilon_a)]^2$ (fig. 4a). As V_0 increases to larger values, $R^+(t=0)$ approaches the asymptotic value of 0.5.

As implied above, the analytic expression for R^+ in eq. (2) should only be valid for small V_0. The values of R^+ determined by numerically integrating eq. (11) for the two-level model are shown in fig. 5a. Also plotted are the values of R^+ determined from eq. (2) for two of the V_0 values. As expected, the agreement between the numerical and analytic R^+ values are best for $V_0 \leqslant 0.05$ eV. In the low velocity regime, then, $R^+ \propto v^2$. For large V_0 ($\geqslant 0.4$ eV), the values of R^+ at low velocities decrease with V_0 rather than increase as V_0^2. Even though R^+ is not proportional to V_0^2 at low velocities, it does remain proportional to v^2.

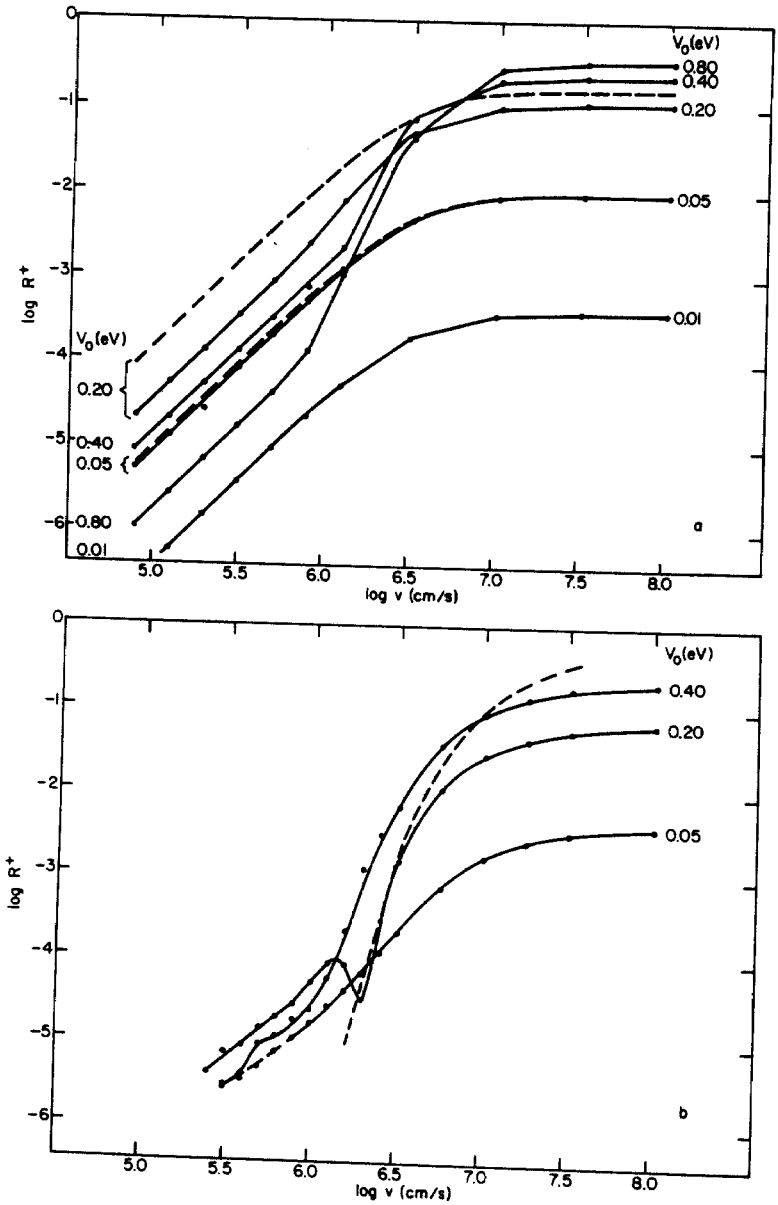

Fig. 5. (a) Log R^+ versus log v for various values of V_0 of the two-level model. The value of $(\epsilon_i - \epsilon_a)$ is 0.5 eV and $\lambda = 2.3$ Å^{-1}. The dashed lines are calculated from eq. (2) with the same parameters. For $V_0 = 0.01$ eV, the analytic and numerical curves are identical. (b) Log R^+ versus log v for various values of V_0 of the metal–adsorbate interaction in the multilevel model. In all cases the value of V_0 for the metal–metal interaction is 0.20 eV. The electronic zone F is used. The dashed line is calculated from eq. (6) with $(IP - \phi) = 0.9$ eV and $C_1 = 1$.

In the multilevel system, since the atoms in the solid do not move a significant distance, the influence of the metal–metal V_0 value on R^+ is not investigated. Unlike the situation which exists for the two-level analytic models, the analytic expression given in eq. (3) derived with an infinite number of levels exhibits no dependence of R^+ on V_0. However, as seen in fig. 5b, R^+ is found to be V_0-dependent in a manner similar to that found for the two-level systems.

The values of R^+ predicted by eq. (6) are shown as a dashed line in fig. 5b for $(\mathrm{IP}-\phi)=0.9$ eV, which is a reasonable energy difference between the adsorbate energy of -6.0 eV and the lowest band of unoccupied levels at -5.1 eV. The value of the parameter C_1 is set to 1. In the velocity regime between 10^6 and 10^7 cm/s, the dependence of R^+ on v more nearly approaches $\exp(-\mathrm{const}/v)$ especially for the larger values of V_0. The predicted value of R^+ at $v=10^{5.5}$ cm/s using eq. (6), however, is $\sim 10^{-26}$. It is interesting to note that eq. (6) was derived for ion scattering from surfaces where (i) the velocity range of interest is greater than 10^6 and probably 10^7 cm/s, (ii) the initial condition (i.e., the initial charge on the "adsorbate") is 0 or 1 and not a partial charge, and (iii) V_0 is assumed to be large [15]. This behavior of R^+ for larger values of V_0 is also observed in the two-level model and shown in fig. 5a. As noted above, R^+ more closely approximates $\exp(-\mathrm{const}/v)$ for larger V_0 values both in the two-level and multilevel systems. This observation is consistent with assumptions utilized to derive eq. (6) since its precursor formula contained the transition probability or level broadening Δ, where

$$\Delta \propto V_0^2, \tag{15}$$

and Δ was assumed to be large [15]. The results presented here indicate that when V_0 is large an exponential dependence of R^+ on velocity is also expected.

4.3. R^+ *versus* λ

The parameter λ (or $1/\lambda$) measures the effective range of the electronic interaction between the ejected particle and the solid. As λ between the metal levels and the adsorbate level increases or the interaction range decreases, the ionization probability tends toward the initial charge (fig. 6). For large interaction ranges (small λ) there is a greater probability of electron transfer from the substrate levels to the adsorbate level, thus the value of R^+ is smaller. For velocities $\leqslant 10^6$ cm/s, R^+ is approximately proportional to λ^2 in both the two-level and multilevel models.

In addition to varying the metal–adsorbate λ we also changed the metal–metal λ to 3.0 Å^{-1} in the multilevel system while keeping the metal–adsorbate λ at 2.3 Å^{-1}. These calculations resulted in the same values of R^+ as with a value of the metal–metal λ of 2.3 Å^{-1} (fig. 6b). For this desorption process then the effect of the electron transfer between the metal atoms is negligible.

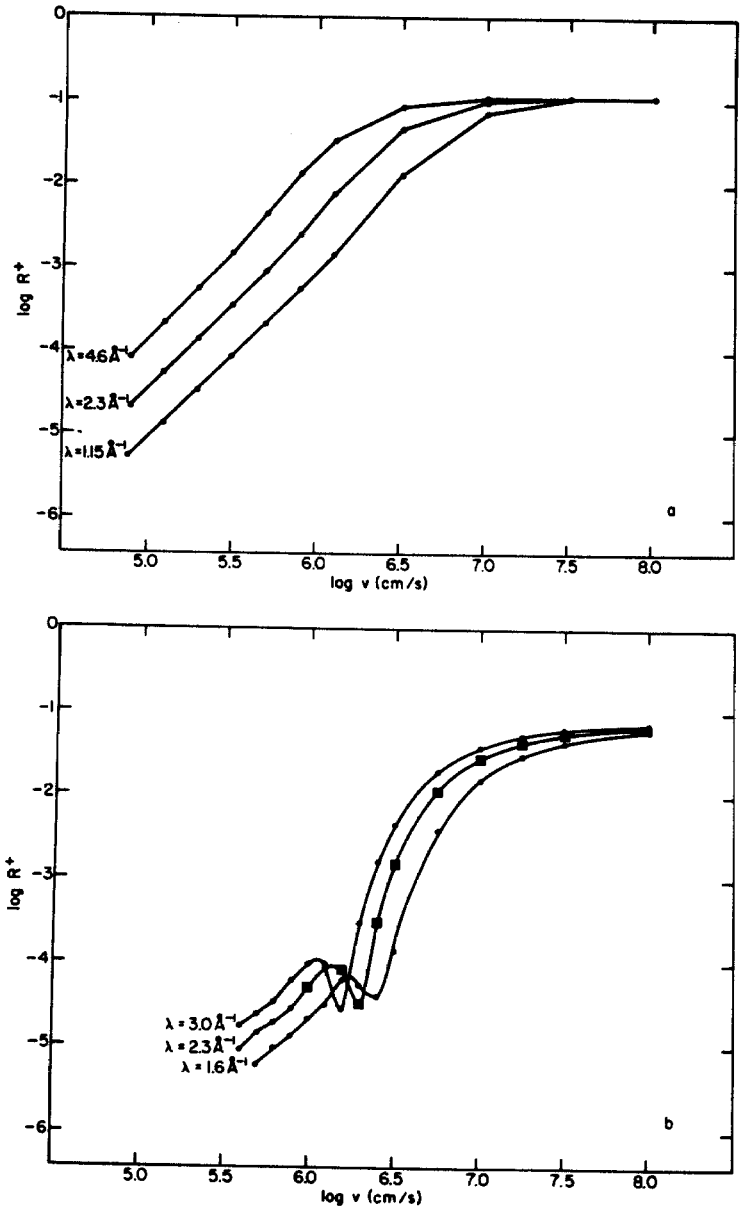

Fig. 6. (a) Log R^+ versus log v for various values λ in the two-level model. The value of $(\epsilon_i - \epsilon_a)$ is 0.5 eV and $V_0 = 0.20$ eV. (b) Log R^+ versus log v for various values of λ of the metal–adsorbate interaction of the multilevel model. For the solid curves the value of λ of the metal–metal interaction is 2.3 $Å^{-1}$. The electronic zone F is used. The squares are the results of calculations where the metal–adsorbate λ is 2.3 $Å^{-1}$ and the metal–metal λ is 3.0 $Å^{-1}$.

4.4. R^+ versus ϵ_a

For the two-level model the energy difference between the two levels influences the initial partial charge on the adatom. Shown in fig. 4b is the value of the initial charge on the adatom plotted as a function of the energy difference $(\epsilon_i - \epsilon_a)$. For the assumption that $R^+(t=0)$ is small to be valid, $(\epsilon_i - \epsilon_a)$ must be greater than approximately 0.5 eV. To increase the probability that the numerical results would agree with eq. (2), we first varied $(\epsilon_i - \epsilon_a)$ for V_0 equal to 0.01 eV. These results are shown in fig. 7 for different values of the velocity. The prediction of eq. (2) for a velocity of $10^{5.7}$ cm/s is shown as a dashed line in fig. 7. The agreement is excellent for $(\epsilon_i - \epsilon_a) \geq 0.5$ eV and quite good for $(\epsilon_i - \epsilon_a) \geq 0.1$ eV. For degenerate levels of $(\epsilon_i - \epsilon_a) = 0$, $R^+ = 0.5$ regardless of the values of v, V_0 or λ. This corresponds to a case which is analogous to the dissociation of H_2^+, where the probability of one H atom having the electron is one half.

As the coupling strength V_0 increases, the value of R^+ does not vary as smoothly with changes in $(\epsilon_i - \epsilon_a)$ as observed for small values of V_0. For V_0 equal to 0.20 eV the log R^+ versus $(\epsilon_i - \epsilon_a)$ curves are shown in fig. 8. For low

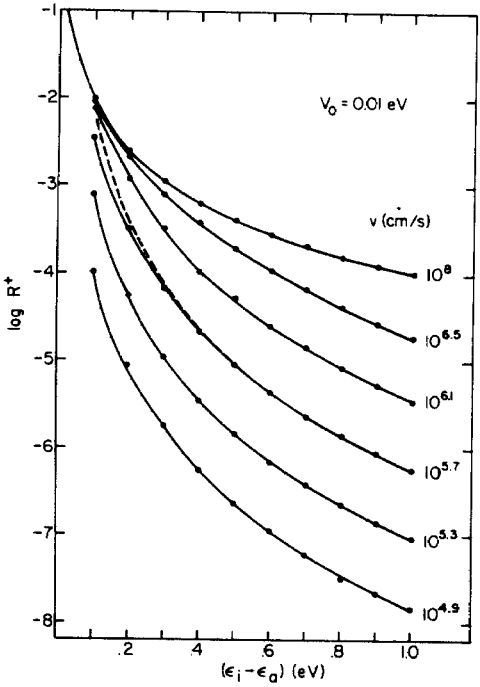

Fig. 7. Log R^+ versus $(\epsilon_i - \epsilon_a)$ for various velocities in the two-level model. The value of V_0 is 0.01 eV and λ is 2.3 $Å^{-1}$. The dashed line is calculated from eq. (2) for a velocity of $10^{5.7}$ cm/s.

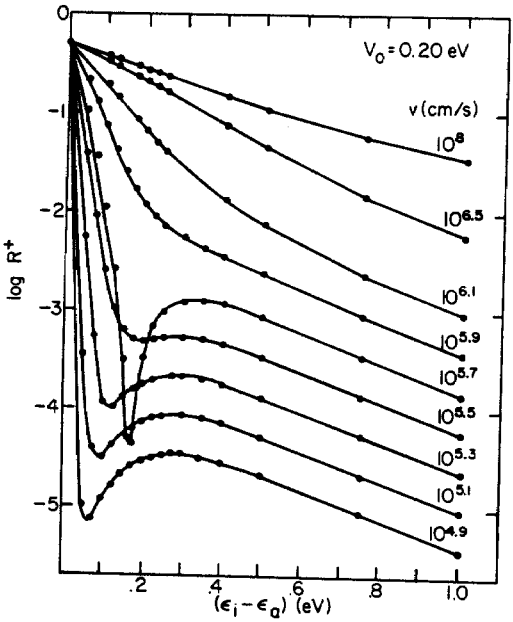

Fig. 8. Log R^+ versus $(\epsilon_i - \epsilon_a)$ for various velocities of the the two-level model. The value of V_0 is 0.20 eV and $\lambda = 2.3$ Å^{-1}.

velocities, there is a minimum in R^+ at small values of $(\epsilon_i - \epsilon_a)$. The reasons for this effect may be understood by examining R^+ versus time for a given velocity using the analytic two-level model. For this case [9]

$$R^+(t) = \frac{V_0^2 v^2 \hbar^2}{(\hbar\omega)^2\left[\hbar^2 v^2 \lambda^2 + (\hbar\omega)^2\right]}\left(\lambda^2 + \frac{2\lambda\omega}{v} e^{-\lambda v t} \sin \omega t + \frac{\omega^2}{v^2} e^{-2\lambda v t}\right), \quad (16)$$

where $\hbar\omega = \epsilon_i - \epsilon_a$. This formula has also been derived independently by Diestler using the molecular orbital basis [24]. For $t \to \infty$, eq. (16) is identical to eq. (2). For $t = 0$, eq. (16) predicts that $R^+(t=0) = V_0^2/(\hbar\omega)^2$. The assumption by both Sroubek and Diestler in the derivations of eqs. (2) and (16) is that $R^+(t=0)$ is small. Shown in fig. 9a is the value of $R^+(t)$ from the numerical integration of eq. (11) for a velocity of $10^{5.9}$ cm/s and four values of $(\epsilon_i - \epsilon_a) = \hbar\omega$ with $V_0 = 0.20$ eV. Although eq. (16) does not yield the same values of $R^+(t)$ for this case since V_0 is too large, it does predict the qualitative characteristics of $R^+(t)$. Because of the sin ωt term in eq. (16), oscillatory behavior at a frequency ω is predicted in the charge exchange process. This corresponds to transfer of the electron density back and forth between the adatom and the substrate. Thus it is difficult to view this overall process as

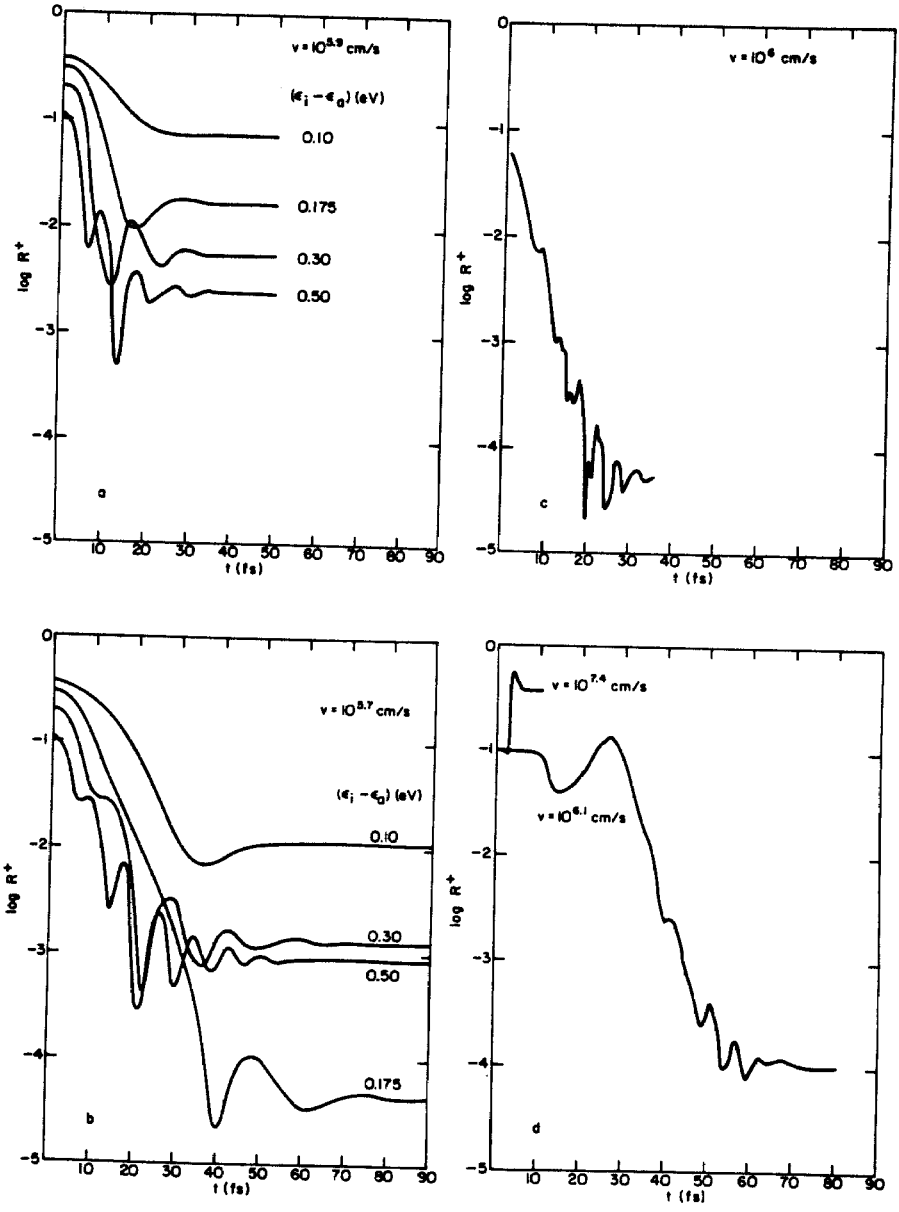

Fig. 9. Log R^+ versus time. The values of the parameters are $V_0 = 0.20$ eV and $\lambda = 2.3$ Å^{-1}. The curves were obtained from the numerical integration of eq. (11) (1 fs $= 10^{-15}$ s): (a) $v = 10^{5.9}$ cm/s for the two-level model; (b) $v = 10^{5.7}$ cm/s for the two-level model; (c) $v = 10^6$ cm/s for the multilevel model, $\epsilon_a = -6.0$ eV; (d) $v = 10^{6.1}$ and $10^{7.4}$ cm/s for the multilevel model with motion in the solid, $\epsilon_a = -5.8$ eV.

either "ionization" or "neutralization", although the net effect in this case is that the adatom becomes more neutral. The period of this charge transfer is well approximated by $\tau \simeq 2\pi/\omega$, independent of λ and v. The magnitude of the oscillations, however, depends on λ and the ratio ω/v. Similar oscillations have been found by other workers for the ion scattering process [14].

The analogous curves for a velocity of $10^{5.7}$ cm/s are shown in fig. 9b. For $\hbar\omega = 0.10$, 0.30 and 0.50 eV, the curves of $R^+(t)$ versus time are very similar to those for a velocity of $10^{5.9}$ cm/s (fig. 9a). For the energy of the minimum ($\hbar\omega = 0.175$ eV) in the R^+ versus $(\epsilon_i - \epsilon_a)$ curve of fig. 8, the first minimum in fig. 9b is missing or is at least suppressed. This anomalous or resonance behavior occurs when $\omega/v \simeq 2\lambda$ and all the terms in eq. (16) are comparable in magnitude. Although these large variations of R^+ with changing $(\epsilon_i - \epsilon_a)$ or v appear quite important in this two level model, their influence can average out when more levels are added to the solid. As seen in fig. 9c, the oscillatory regular behavior is not nearly so pronounced in the values of $R^+(t)$ versus t for a system with many electronic levels.

In the multilevel system, the effect on the values of R^+ of changing the energy ϵ_a of the adsorbate level (the ionization potential, IP), is qualitatively similar (fig. 10) to that observed in the two-level case. At high velocities the value of R^+ decreases as ϵ_a is lowered or as the IP is raised. At lower velocities,

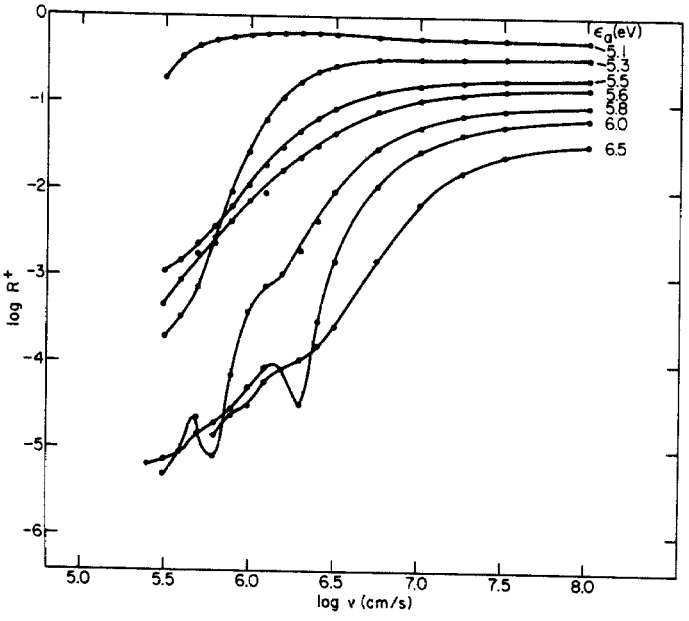

Fig. 10. Log R^+ versus log v in the multilevel model for various values of $(-\epsilon_a)$. In all cases, $V_0 = 0.20$ eV, $\lambda = 2.3$ Å^{-1}, $\epsilon_{1,2} = -5.0$ and -5.5 eV.

however, resonance effects begin to affect R^+ and there is no longer a smooth dependence of R^+ on ϵ_a. In the two-level case, if the levels are degenerate, $R^+ = 0.5$ and is independent of velocity. From fig. 10 it is seen that R^+ is independent of velocity for $\epsilon_a \simeq -5.1$ eV.

The resonance type behavior is exhibited in the multilevel calculation as well as the two-level calculation. It is noticable in the R^+ versus ϵ_a curves (fig. 10), the R^+ versus v curves (fig. 3) and the R^+ versus λ curves (fig. 6b). As discussed above, the velocity at which the resonance occurs correlates with ω/λ. As seen in fig. 6b, as λ increases, the velocity at which the minimum in R^+ occurs decreases. Note also that by changing the electronic zone from E to F in fig. 3a, the minimum at $v = 10^{6.2}$ cm/s disappears. This resonance type behavior in the plot of log R^+ versus log v then is due to discrete energy levels and might not be observed experimentally for a system with a dense spectrum of metal levels and where the ions that desorb at one velocity correspond to an average of many types of motion in the solid. There is always the possibility, however, as in the case of He^+ scattering from Pb, that these resonance effects can be observed [14a,32].

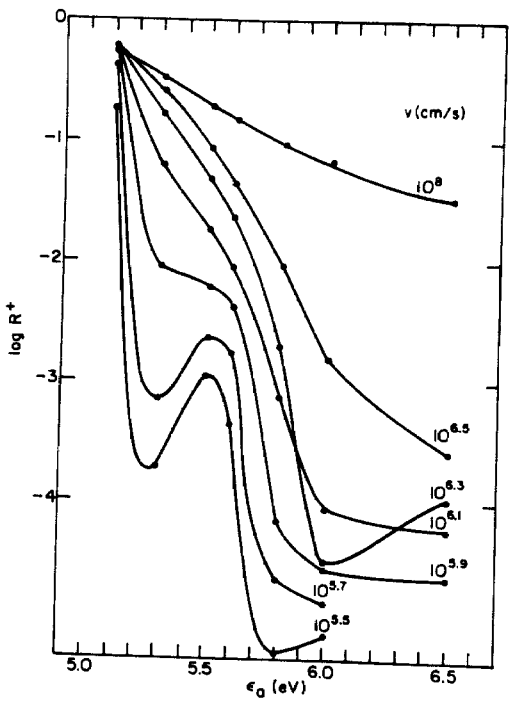

Fig. 11. Log R^+ versus ϵ_a in the multilevel model for various velocities. $V_0 = 0.20$ eV, $\lambda = 2.3$ Å^{-1}, $\epsilon_{1,2} = -5.0$ eV and -5.5 eV in all cases.

Experimentally a linear correlation has been obtained between log R^+ and the IP of the desorbing species. Shown in fig. 11 are the values of log R^+ versus ϵ_a for several values of the velocity. There is not an obvious linear relationship between R^+ and ϵ_a. Due to the resonance type effects discussed above, the curves for some of the values of velocity, e.g., $v = 10^{6.3}$ cm/s, cross. However, the slopes of the log R^+ versus ϵ_a curves as predicted by eq. (5) reasonably approximate the ones shown in fig. 11 if the oscillations are smoothed over.

4.5. Alternate $V(t)$ and particle motion

Obviously two assumptions in the results presented above are the precise form of the electronic coupling $V(r(t))$ and the restricted set of motions of the ejected adatom. Although the exponential form of $V(r(t))$ in eq. (12) is physically reasonable, mathematically it has a cusp at $t = 0$. To remove this feature, we used an alternate $V(r(t))$ that is proportional to sech $(1.65\lambda\, r(t))$ [20]. Shown in fig. 12 are the predicted values of R^+ for both the exponential and sech forms of the coupling integral. The curves are reasonably similar.

Ultimately it is desirable to use this model to describe the electronic processes involved in the desorption of particles due to collision cascades that originate from within the solid. As a first step towards modeling these types of

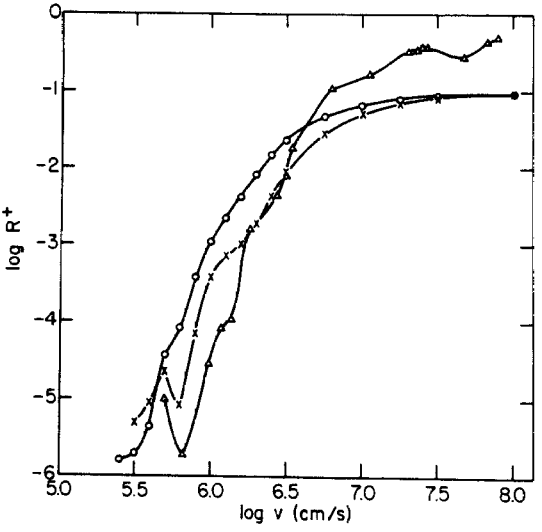

Fig. 12. Log R versus log v in the multilevel model. $V_0 = 0.20$ eV, $\lambda = 2.3$ Å^{-1}, $\epsilon_{1,2} = -5.0$ and -5.5 eV, $\epsilon_a = -5.8$ eV; (×) for desorption, using the exponential form of the coupling integral; (○) for desorption, using the sech form of the coupling integral; (△) for desorption with motion in the solid.

processes, a particle is used to strike the second layer copper atom that is directly below the adatom. This copper atom then collides with the adatom forcing it to desorb. This process allows for the adatom to smoothly initiate its motion rather than having a discontinuous velocity change. This motion also differs from the desorption calculation in that the copper atom and the adatom approach each other at a distance smaller than r^c before they move apart. As shown in fig. 12, for velocities less than $\sim 10^{6.5}$ cm/s the predicted values of R^+ for the atom motion case are very similar to those from the desorption case. The local minimum at $v \approx 10^{5.7}$ cm/s is even observed for both curves. At high velocities the value of R^+ for the motion case is larger than in the desorption case. This can be qualitatively understood by examining the dependence of R^+ on time. Shown in fig. 9d are the values of $R^+(t)$ versus t for two different final velocities of the ejected adatom, $10^{6.1}$ cm/s and $10^{7.4}$ cm/s. For $v = 10^{6.1}$ cm/s, $R^+(t)$ initially decreases as the time increases to 12 fs. At this time the adatom has not moved, but the second layer copper atom is moving toward the first layer. Between a time of 13 and 25 fs the copper atom begins to strike the adatom with the point of closest encounter at $t \approx 25$ fs. During this time period $R^+(t)$ increases. After ~ 26 fs both the adatom and the copper atom desorb with the adatom having the larger velocity, thus it moves away from both the surface and the copper atom. The $R^+(t)$ versus t curve for $t > 25$ fs is very similar to fig. 9c for the desorption of an adatom with similar velocity.

In the high velocity regime (fig. 9d for $v = 10^{7.4}$ cm/s) as the copper atom moves toward the first layer there is a small decrease in the values of R^+. As the collision proceeds the value of R^+ increases. At this stage the adatom leaves the surface with a high velocity, retaining the charge that is attained during the collision with the copper atom. For this high velocity, the ionization probability is actually greater than the initial charge.

5. Conclusions

In developing a microscopic model to describe the charge transfer process at surfaces, a system of an atom desorbing perpendicular to the surface has been analyzed in detail. Since this system can be solved analytically with certain approximations, this affords the opportunity to understand the severity of the approximations as well as to understand the simplest situation before complicating the process further by adding motion of atoms in the solid. For the choice of parameters examined here we find at velocities appropriate for ion bombardment studies that the ionization probability R^+ is proportional to v^n where n is between 2 and 4. Under conditions where the interaction between the atomic levels (V_0) is large however, R^+ may depend more exponentially on $(-\text{const.}/v)$.

This model appears very promising as a means of examining the charge transfer at surfaces. There are many more aspects to investigate, however, before a final conclusion can be reached on its applicability and generality. A larger range of parameters needs to be tested. These include the parameters varied in this study as well as an almost infinite variety of motions within the solid that give rise to the desorption of an atom. In particular, for the angle resolved SIMS, ESD and PSD experiments, the dependence of R^+ on angle of the ejected atom is crucial. The influence of the binding energy, since this causes the atom to desorb with a non-constant velocity, on the ionization process also needs to be understood. Finally, it will be desirable to extend this models to describe the formation of negative ions.

Acknowledgments

Partial support for these studies is gratefully acknowledged from the Office of Naval Research and the National Science Foundation. We also thank the Alfred P. Sloan Foundation for a Research Fellowship and the Camille and Henry Dreyfus Foundation for a grant for newly appointed young faculty. This work could not have succeeded without helpful discussions from many people including D.J. Diestler, N. Winograd, W. Steele, J. Tully and D. Hone.

Note added in proof

Dr. A.R. Krauss kindly pointed out an additional reference where there is experimental evidence for a power law dependence of R^+ on velocity. In ref. [33], the authors find for beryllium ions ejected that R^+ is proportional to v^n, where $n = 2$–3. They also observe a binding energy effect at low velocities. This work is in qualitative agreement with the conclusions presented here.

References

[1] A. Benninghoven, Surface Sci. 53 (1975) 596.
[2] B.J. Garrison and N. Winograd, Science 216 (1982) 805;
N. Winograd, Progr. Solid State Chem. 13 (1982) 285.
[3] R.A. Gibbs, S.P. Holland, K.E. Foley, B.J. Garrison and N. Winograd, Phys. Rev. B24 (1981) 6178; J. Chem. Phys. 76 (1982) 684.
[4] T.E. Madey and J.T. Yates, Jr., Chem. Phys. Letters 51 (1977) 77.
[5] P. Eisenberger and L.C. Feldman, Science 214 (1981) 300.
[6] H.H. Brongersma and J.B. Theeten, Surface Sci. 54 (1976) 519.
[7] N. Winograd, D.E. Harrison, Jr. and B.J. Garrison, Surface Sci. 78 (1978) 467;
B.J. Garrison, N. Winograd and D.E. Harrison, Jr., Phys. Rev. B18 (1978) 6000;

N. Winograd, B.J. Garrison and D.E. Harrison, Jr., J. Chem. Phys. 73 (1980) 3473;
B.J. Garrison, J. Am. Chem. Soc. 104 (1982) 6211.
[8] P. Williams, Surface Sci. 90 (1979) 588.
[9] T. Lundquist, J. Vacuum Sci. Technol. 15 (1978) 684.
[10] M.L. Yu, Phys. Rev. Letters 47 (1981) 1325.
[11] N. Winograd, J.P. Baxter and F. Kimock, Chem. Phys. Letters 88 (1982) 581.
[12] N.H. Tolk and and J.C. Tully, in: Inelastic Ion–Surface Collisions (Academic Press, New York, 1977) p. 105.
[13] S. Kapur, and B.J. Garrison, J. Chem. Phys. 75 (1981) 445; Surface Sci. 109 (1981) 435.
[14] (a) J.C. Tully, Phys. Rev. B16 (1977) 4324;
(b) Y. Muda and T. Hanawa, Surface Sci. 97 (1980) 283;
(c) K.L. Sebastian, V.C. Jyothi Bhasu and T.B. Grimley, Surface Sci. 110 (1981) L571;
(d) H.K. McDowell, J. Chem. Phys. 77 (1982) 3263.
[15] A. Blandin, A. Nourtier and D. Hone, J. Physique 37 (1976) 369;
W. Bloss and D. Hone, Surface Sci. 72 (1978) 277.
[16] R. Brako and D.M. Newns, Surface Sci. 108 (1981) 253.
[17] E.G. Overbosch and J. Los. Surface Sci. 108 (1981) 99, 117.
[18] Z. Sroubek, Surface Sci. 44 (1974) 47.
[19] Z. Sroubek, J. Zavadil, F. Kubec and K. Zdansky, Surface Sci. 77 (1978) 603.
[20] Z. Sroubek, in: Inelastic Particle–Surface Collisions, Springer Series in Chemical Physics, Vol. 17, Eds. E. Taglauer and W. Heiland (Springer, Berlin, 1981) p. 277.
[21] J.K. Nørskov and B.I. Lundqvist, Phys. Rev. B19 (1979) 5661.
[22] Z. Sroubek, K. Zdansky and J. Zavadil, Phys. Rev. Letters 45 (1980) 580.
[23] L.I. Schiff, Quantum Mechanics (McGraw-Hill, New York. 1968) p. 282.
[24] D.J. Diestler, to be published.
[25] Z. Sroubek obtained a similar dependence of R^+ on velocity in the two-level model by using $V(t) = V_0/\cosh(\lambda v t)$. These results were obtained, however, by assuming that the adatom was brought up to surface at the same speed v at which it desorbs. Numerical integration of the Diestler perturbation model using the hyperbolic cosine form of $V(t)$ yields values R^+ that are approximately proportional to v^4.
[26] C.A. Andersen and J.R. Hinthorne, Anal. Chem. 45 (1973) 1421.
[27] J.C. Tully, in: Dynamics of Molecular Collisions, Part B. Ed. W.H. Miller (Plenum, New York, 1976).
[28] D.E. Harrison, Jr., W.L. Gay and H.M. Effron, J. Math. Phys. 10 (1969) 1179.
[29] B.J. Garrision, in: Potential Energy Surfaces and Dynamics Calculations for Chemical Reactions and Molecular Energy Transfer, Ed. D.G. Truhlar (Plenum, New York, 1981).
[30] W.H. Miller and T.F. George, J. Chem. Phys. 56 (1972) 5668.
[31] J.-H. Lin and B.J. Garrison, J. Vacuum Sci. Technol., in press.
[32] R.L. Erickson and D.P. Smith, Phys. Rev. Letters 34 (1975) 297;
N.H. Tolk, J.C. Tully , J. Kraus, C.W. White and S.N. Neff, Phys. Rev. Letters 36 (1976) 747.
[33] A.R. Krauss and D.M. Gruen, Surface Sci. 92 (1980) 14.